Implementation of Snowpack Treatment in the CPC Water Balance Model and Its Impact on Drought Assessment

JORGE AREVALO,[a,b] JOSH WELTY,[a] YUN FAN,[c] AND XUBIN ZENG[a]

[a] *Department of Hydrology and Atmospheric Sciences, The University of Arizona, Tucson, Arizona*
[b] *Departamento de Meteorologia, Universidad de Valparaiso, Valparaiso, Chile*
[c] *NOAA/National Weather Service/National Centers for Environmental Protection/Climate Prediction Center, Camp Springs, Maryland*

(Manuscript received 10 August 2020, in final form 5 March 2021)

ABSTRACT: Droughts are a worldwide concern, thus assessment efforts are conducted by many centers around the world, mainly through simple drought indices, which usually neglect important hydrometeorological processes or require variables available only from complex land surface models (LSMs). The U.S. Climate Prediction Center (CPC) uses the Leaky Bucket (LB) water-balance model to postprocess temperature and precipitation, providing soil moisture (SM) anomalies to assess drought conditions. However, despite its crucial role in the water cycle, snowpack has been neglected by LB and most drought indices. Taking advantage of the high-quality snow water equivalent (SWE) data from The University of Arizona (UA), a single-layer snow scheme, forced by daily temperature and precipitation only, is developed for LB implementation and tested with two independent forcing datasets. Compared against the UA and SNOTEL SWE data over CONUS, LB outperforms a sophisticated LSM (Noah/NLDAS-2), with the median LB versus SNOTEL correlation (RMSE) about 40% (26%) higher (lower) than that from Noah/NLDAS-2, with only slight differences due to different forcing datasets. The changes in the temporal variability of SM due to the snowpack treatment lead to improved temporal and spatial distribution of drought conditions in the LB simulations compared to the reference U.S. Drought Monitor maps, highlighting the importance of snowpack inclusion in drought assessment. The simplicity but reasonable reliability of the LB with snowpack treatment makes it suitable for drought monitoring and forecasting in both snow-covered and snow-free areas, while only requiring precipitation and temperature data (markedly less than other water-balance-based indices).

KEYWORDS: Drought; Snowpack; Hydrometeorology; Soil moisture; Land surface model

1. Introduction

Droughts are one of the more widespread natural disasters affecting society. Their impacts extend to ecosystems, agriculture, industrial production, power generation, and water for human consumption, with societal effects even beyond the directly affected area or after its recovery (Mishra and Singh 2010; Sutanto et al. 2019; Van Loon 2015). Furthermore, increased temperatures and evapotranspiration demand will lead to more frequent droughts lasting for longer periods with subsequent larger societal impacts (Naumann et al. 2018; Mukherjee et al. 2018; Trenberth et al. 2014; Dai and Zhao 2017). Hence development and improvement of drought assessment tools would benefit the entire society.

However, the lack of a universal definition of drought is one of the biggest obstacles in its assessment (Lloyd-Hughes 2014; Wilhite and Glantz 1985; Mishra and Singh 2010). Historically, droughts have been classified in different types, such as meteorological, hydrological, agricultural, groundwater, and socioeconomic droughts (Mishra and Singh 2010; Bloomfield and Marchant 2013; Thomas et al. 2017). For this reason, a large set of indices and frameworks for drought assessment have been developed depending on the hydrometeorological or environmental variables of interest, each with unique strengths and weaknesses (Heim 2002; Mishra and Singh 2010).

Among the hydrometeorological variables, soil moisture (SM) is a very suitable one for assessing drought conditions, as it incorporates antecedent conditions and recent precipitation, indicates the water storage available for vegetation, and even impacts the streamflow (Sheffield et al. 2004). However, accurate soil moisture measurements are usually scarce, thus many of the most commonly used drought indices account only for precipitation, e.g., the standardized precipitation index (SPI; McKee et al. 1993). Conversely, much more comprehensive approaches have also been developed to account for more terms in the water balance, generally relying on simulated quantities from land surface models (LSMs), such as the soil moisture deficit index (SMDI; Narasimhan and Srinivasan 2005) or the standardized moisture anomaly index (SZI; Zhang et al. 2015, 2019).

Although comprehensive indices overcome several of the known deficiencies of the simpler ones, they also introduce uncertainties present in the suite of variables needed. However, they usually lack the flexibility provided by intermediate indices to be fed with more accessible data (usually precipitation and temperature), such as the Palmer drought severity index (PDSI; Palmer 1965), which uses a simplified water balance to account for the moisture anomaly index. This flexibility is particularly important, for instance, for drought forecasting at seasonal and

Supplemental information related to this paper is available at the Journals Online website: https://doi.org/10.1175/JHM-D-20-0201.s1.

Corresponding author: Jorge Arevalo, jorgearevalo@email.arizona.edu

DOI: 10.1175/JHM-D-20-0201.1

subseasonal scales, when the most reliable predictions are often the result of postprocessing of dynamic models, statistical estimations, and/or more recently machine learning models. Furthermore, such predictions are typically available for just a small number of variables, not necessarily including the full suite required by the complex drought indices.

The PDSI is physically based and requires only precipitation and temperature, and is therefore among the most widely used drought indices around the globe. However, it still has some important caveats (Zhang et al. 2015), including the oversimplification of the hydrological model, the high sensitivity to the parameter calibration, its fixed temporal scale, and the lack of snowpack treatment, among others. In the same spirit, the Climate Prediction Center (CPC) from the National Oceanic and Atmospheric Administration (NOAA) uses their Leaky Bucket (LB) water balance model (Huang et al. 1996; van den Dool et al. 2003) to assess drought as their contribution to the U.S. Drought Monitor (U.S.-DM; Svoboda et al. 2002). The drought assessment is performed through the analysis of soil moisture at a different range of temporal and spatial scales, derived from the postprocessing of gridded temperature and precipitation via the LB. The simplicity of this model and its reasonable performance allow the CPC to assess drought conditions by forcing LB with several different input datasets, including gridded observation-based data, land surface model outputs, and corrected numerical weather forecasts and climate predictions, for both monitoring and forecasting. However, LB still shares some of the same caveats as the PDSI.

Snowpack acts as a natural reservoir of water, introducing a delay between the winter snowfall and the water availability during spring or summer, impacting the annual cycle of soil moisture, surface streamflow, and even groundwater. It also acts as an insulator of the soil, preventing the evaporation of moisture from the underlying ground. Through these impacts, snowpack not only affects the current availability of water, but also the reference climatology of soil moisture and streamflow. In snow dominated basins, years with below normal maximum snow water equivalent (SWE) can result in earlier summer low-flow occurrences, coinciding with below normal minimum streamflow (Jenicek et al. 2016) and soil moisture storage. However, if SWE deficits occur due to warmer winter temperatures (warm snow drought), as opposed to below normal winter precipitation (dry snow drought), smaller snow accumulation can be related to the lower ratio of snowfall to total precipitation and/or quicker snow melting (Harpold et al. 2017a; Blahušiaková et al. 2020). Such differences in snowpack dynamics have diverse impacts on reservoir operations, requirement and availability of water for irrigation, and ecosystem functioning, including increased wildfire risk (Westerling et al. 2006).

Despite the recognized impact of snowpack on the water balance, and consequently droughts (e.g., Van Loon and Van Lanen 2012; Staudinger et al. 2014; Zhang et al. 2019; Trenberth et al. 2014), it has been usually neglected in the drought assessment, including the CPC-LB. Thus, some efforts have been taken to develop new drought indices accounting for snow processes. Staudinger et al. (2014) proposed an extension to SPI, the standardized snowmelt and rain index (SMRI), requiring only temperature and precipitation to derive snowmelt by means of a simple degree-day snow model. Zhang et al. (2019) added snow processes to the standardized moisture anomaly index (SZI; Zhang et al. 2015) but require additional variables, including snow water equivalent (SWE), from very complex LSMs. Huning and AghaKouchak (2020) performed a global analysis of snow drought using the SWEI, a standardized drought index directly using SWE data. Before these recent studies, very few indices accounting for snow were developed (e.g., Doesken et al. 1991), mostly due to the lack of snow data.Recently, the University of Arizona (UA) released a very high-quality snow dataset (Broxton et al. 2019) at 4-km resolution over the conterminous United States (CONUS), with daily data from 1982 to the present. This dataset passed several quality-control tests (Broxton et al. 2016a,b; Dawson et al. 2018), including comparisons with SWE from the Snowpack Telemetry (SNOTEL) network and an independent comparison with gamma-ray SWE (Cho et al. 2020), positioning it as a reliable gridded dataset for SWE and snow depth over CONUS. This dataset, in conjunction with the high-quality PRISM dataset for precipitation and temperature, allows us to more precisely explore the relationships between temperature, precipitation, snowfall and snow ablation, at daily scale.

Recognizing the importance of simple tools for drought assessment, requiring only commonly available variables while at the same time accounting for the most important water balance terms, the main goal of this study is to improve the drought assessment in the CPC through the development and implementation of a snowpack scheme within the LB. To that end, we will first evaluate the performance of the snow scheme, second assess its impact on soil moisture, and last test if this improves the drought assessment.

2. Methods

a. Data

We use the UA 4-km daily SWE dataset (Broxton et al. 2019) from January 1982 to December 2016 over CONUS (Broxton et al. 2016a; Dawson et al. 2017; Zeng et al. 2018) to guide the snow scheme development (October 1984–September 1989) and for SWE evaluation of the LB simulations (with snowpack treatment; October 1994–September 1999, and October 2005–September 2010). This dataset incorporates all the available data from the Snow Telemetry (SNOTEL) network of the Natural Resources Conservation Service (NRCS) and from the Cooperative Observer Network (COOP), as well as temperature and precipitation from the PRISM Climate Group.

The high quality of this product and its advantages over other available datasets have been demonstrated in the past through rigorous tests, including point-to-point interpolation (Broxton et al. 2016a), point-to-pixel interpolation (Broxton et al. 2016b), comparison against independent snow cover extent and airborne lidar measurements (Dawson et al. 2018), and an evaluation against Gamma SWE (Cho et al. 2020) performed by an independent research group. Hence, the UA SWE dataset will be used as the ground truth for SWE. Furthermore, data from the SNOTEL network for more than

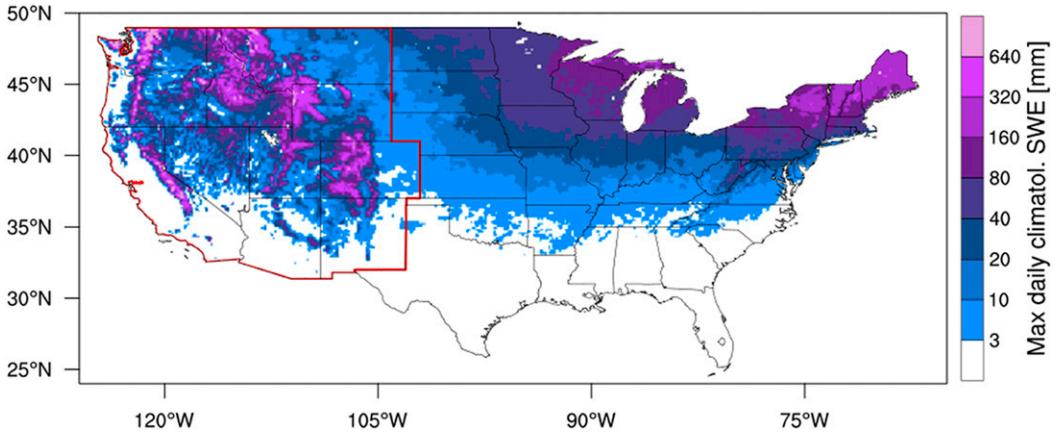

FIG. 1. Area of study (conterminous United States). The red polygon encloses the WEST domain. The maximum daily SWE climatology (1982–2016) is shown, as obtained from the LB simulation (with CPC forcing data and snowpack treatment). Grids with values lower than 3 mm are masked out.

650 stations are also used for evaluation of LB SWE and for reference comparison against the North American Land Data Assimilation System version 2 (Noah/NLDAS-2) and the UA product (Fig. S1 in the online supplemental material).

To force LB, two different datasets are employed to test the robustness of the snowpack scheme to the forcing data. They include the daily averaged precipitation and 2-m air temperature prepared by CPC for the 1/8° LB grid from the NLDAS-2 forcing data (Xia et al. 2009), referred to as "CPC forcing data" hereafter, and the PRISM 4-km daily near surface temperature and precipitation (The PRISM Climate Group 2004; Daly et al. 2008) for the same period as the UA-SWE dataset. The PRISM dataset is also used to compliment the UA-SWE in the development of the snow scheme.

For comparison, the 1/8° daily SWE data (represented by the last hourly value of each day) from the NLDAS-2 (Xia et al. 2012a,b) utilizing the Noah2.8 land surface model (LSM) are used. Noah is one of the widely used LSMs and it is utilized by the NOAA National Centers for Environmental Prediction (NCEP) for operational weather and climate prediction. It is driven by precipitation, air temperature, wind, humidity, and downward shortwave and longwave radiation fluxes at each time step (e.g., 30 min), with a detailed representation of most of the water and energy cycle processes.

The percentage areas within each of the five drought categories and the drought status maps for specific dates from January 2000 to present from the U.S.-DM (NDMC/NOAA/USDA 1999; Svoboda et al. 2002) are used as a reference dataset to evaluate the drought condition estimated from the LB soil moisture standardized anomalies. These five categories correspond to abnormally dry (D0), moderate drought (D1), severe drought (D2), extreme drought (D3), and exceptional drought (D4).

All of the above data are regridded using bilinear interpolation to the LB 1/8° grid (Fig. 1). Daily climatologies are computed for each grid from January 1982 to December 2016 and smoothed by retaining only the first six harmonics. To compare the gridded data against the SNOTEL point observations, the values in the nearest pixel to each station are chosen. The timing difference in the day definition between the datasets (i.e., UA SWE and PRISM consider the day centered at midnight while CPC and Noah/NLDAS-2 are centered at noon) is neglected, as it is expected to have a negligible impact on the analyses presented here.

b. Model description

NOAA/NCEP/CPC uses the Leaky Bucket model as a temperature and precipitation postprocessing tool for computing daily soil moisture at 1/8° grids over the CONUS (Huang et al. 1996; van den Dool et al. 2003). The LB is forced with daily precipitation and temperature only, and based on mass conservation of soil moisture W within a single layer of 1.6 m:

$$\frac{dW}{dt} = P - E - R - G, \tag{1}$$

where P is precipitation, E is evapotranspiration (as a function of W and the temperature-dependent potential evapotranspiration), R is surface plus subsurface runoff (depending on P and W), and G is groundwater loss (as a function of W). However, LB does not account for snow processes, which has been recognized as one of its limitations by van den Dool et al. (2003).

To improve the representation of soil moisture in areas with snow, we have developed a one-layer snow scheme with a new prognostic variable, snow water equivalent [SWE (mm)] for LB (referred to as LBS hereafter, with "S" denoting snow). The snow mass conservation at each grid is

$$\frac{\Delta \mathrm{SWE}}{\Delta t} = S - A, \tag{2}$$

where S stands for snowfall (mm day^{-1}) and A for ablation (mm day^{-1}), ΔSWE = SWE(t) − SWE($t - \Delta t$) with a fixed daily time step (Δt). The UA SWE and PRISM P and T data enable us to find general relationships of S and A as functions of P and T. For this purpose, the data were subset to that in the five water years (WYs) from 1985 to 1989 (i.e., 1 October

1984–30 September 1989) over pixels where SWE was at least 5 mm for at least 100 days and the maximum SWE was lower than 300 mm. To develop the parameterization for S, we consider ΔSWE as the snowfall amount (i.e., neglecting the ablation and snow advection) whenever precipitation P is greater than 1 mm and ΔSWE is positive. Figure 2a shows the snowfall fraction of the total precipitation, ΔSWE/P, for those days as a function of T. It can be seen that for T below −1°C, most of the values are close to 1, while for T above 3°C such fraction is close to 0. Hence, we can parameterize S as

$$S = PK_{SF}, \tag{3}$$

$$K_{SF} = \begin{cases} 1, & \text{if} \quad T \le T_{SNOW} \\ \dfrac{T_{RAIN} - T}{T_{RAIN} - T_{SNOW}}, & \text{if} \quad T_{SNOW} < T \le T_{RAIN}, \\ 0, & \text{if} \quad T_{RAIN} < T \end{cases} \tag{4}$$

where K_{SF} is the solid fraction of precipitation, computed with the threshold values $T_{SNOW} = -1.0$°C and $T_{RAIN} = 3.0$°C.

Similarly, for days with $P = 0$ mm day^{-1}, SWE > 0, and SWE in the previous day being at least 30 mm, we identify −ΔSWE as the ablation. From Fig. 2b, ablation for T below −10°C is virtually 0 mm day^{-1}, while above 0°C ablation increases with T. As temperatures slightly above 0°C are more common than the higher ones when snow is present, a quadratic fit was chosen to better represent them. Although ablation is very small for T between −10° and 0°C, it is not negligible as those temperatures are very frequent over snow-covered areas, making the cumulative effect nonnegligible; hence, a linear relationship between T and A was chosen for T in this range. Therefore, we can parameterize A as

$$A = \min\left(A^*, A_{MAX}, \frac{SWE}{\Delta t} + S\right), \tag{5}$$

$$A^* = \begin{cases} 0, & \text{if} \quad T \le T_A \\ \dfrac{A_0(T_A - T)}{T_A}, & \text{if} \quad T_A < T \le 0, \\ aT^2 + bT + A_0, & \text{if} \quad 0 < T \end{cases} \tag{6}$$

where the last term in Eq. (5) is the total SWE available to be melted that day, $A_{MAX} = 20$ (mm day^{-1}) is an overall upper limit, A^* is the potential ablation depending on T in Eq. (6), $T_A = -10$ (°C), $A_0 = 0.2$ (mm day^{-1}), $a = 0.2$ (mm day^{-1} °C^{-2}), and $b = 0.1$ (mm day^{-1} °C^{-1}).

Next, we compute the melting rate M (mm day^{-1}), the input water to the soil P_{input} (mm day^{-1}), and the snowpack constraint on the potential evapotranspiration PE_{LBS} (mm day^{-1}):

$$M = K_{MLT}A, \tag{7}$$

$$P_{input} = (1 - K_{SF})P + M, \tag{8}$$

$$PE_{LBS} = \begin{cases} 0, & \text{if} \quad SWE \ge 1 \\ PE_{LB}, & \text{if} \quad SWE < 1 \end{cases}, \tag{9}$$

where $K_{MLT} = 0.9$.

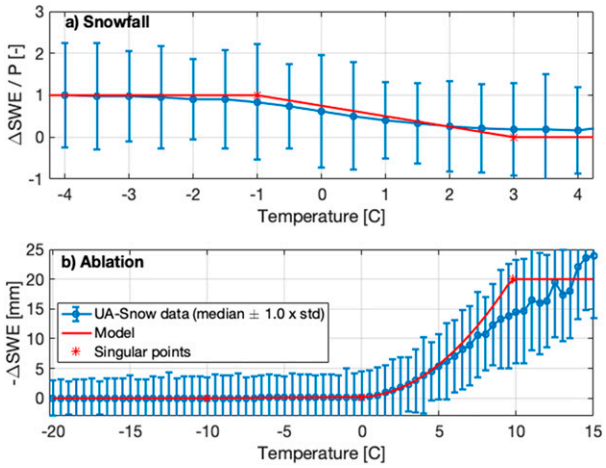

FIG. 2. Estimations of snowfall and ablation functional forms for the LB model. (a) Median [±standard deviation (STD)] of daily SWE increments as fraction of the daily precipitation (ΔSWE/P), presented as a function of temperature, binned every 0.5°C. (b) Median (±STD) of daily SWE decrements (−ΔSWE) as function of temperature, binned every 0.5°C. The red lines represent the functional form chosen for snowfall/ablation in the LBS model. Based on data from UA-SWE and PRISM from 1 Oct 1984 to 30 Sep 1989.

The values for the seven new parameters introduced to LBS were adopted based on the identified relationships from the high-quality available data for the 5-yr period (WY1985–WY1989) over all grid cells within CONUS. They are not tied to any arbitrary geographical or climatological consideration, nor specifically fitted to any individual dataset (e.g., topography). By utilizing data over all of CONUS, across different climate regimes and topography, the expectation is that the scheme will be able to perform adequately on a global scale.

Sensitivity tests were performed for the parameter ranges summarized in the Table S1, where the selected values are also provided. As expected, the scheme is sensitive to the temperature thresholds (T_{SNOW} and T_{RAIN}) in the snowfall parameterization and to the ablation rate at 0°C (A_0). The soil moisture in the LB model is also expected to be sensitive to the melting fraction of the total ablation (K_{MLT}), but the lack of soil moisture measurements in snow-covered areas did not allow us to test and calibrate it.

To keep the snowpack scheme simple and requiring only daily temperature and precipitation, several assumptions are made which partially explain the uncertainty in SWE. Diurnal cycles of temperature and precipitation are neglected, which can lead to biases in the rain/snowfall partitioning. Air humidity is not considered either, which affects the sublimation/melting partitioning, and has also been recognized to impact the rain/snowfall partitioning (Wang et al. 2019; Behrangi et al. 2018; Harpold et al. 2017b). Neglecting the snowpack liquid water content (Techel and Pielmeier 2011), partial melting/refreezing, and energy balance also introduces uncertainty (Samimi and Marshall 2017), particularly for rain

on snow events. The lack of land cover consideration can also limit the ability of the model to correctly represent the snowpack spatial variability. Finally, snowpack dynamics can vary markedly between areas of seasonal versus ephemeral snow (Petersky and Harpold 2018), which is also not explicitly considered here.

LB on its own also has recognized weaknesses, including the assumption of constant soil and other physiographic properties, as well as the lack of a vertical soil profile, energy balance, and diurnal cycle considerations. Additionally, no lateral flow between pixels is considered, preventing the downstream pixels from capturing the runoff (including meltwater) from upstream pixels. Despite all of its limitations, LB has been a useful tool at CPC for decades for drought monitoring (based on observed temperature and precipitation) and prediction (as a simple postprocessing tool of forecasting model output of temperature and precipitation), and for seasonal prediction (using the soil moisture–based analogs), due to its reasonable representation of soil moisture (e.g., Fan and van den Dool 2004; Fan et al. 2011; Fan and Van Den Dool 2011; Wang et al. 2010).

c. *Estimation of drought condition from LB simulated soil moisture*

In an attempt to mimic the U.S.-DM drought categories, soil moisture standardized anomalies (SDAnoms; i.e., difference between actual daily soil moisture and its mean climatology value, normalized by the standard deviation) below −0.5, −0.8, −1.2, −1.5, and −1.9 were related to the categories D0, D1, D2, D3, and D4. It is important to note that the U.S.-DM is a multivariate and more subjective approach to drought monitoring, while the objective categories from LB consider soil moisture only. Hence, the U.S.-DM is taken as a reference, rather than ground truth, in the comparisons presented here.

3. Results and discussion

a. *Snowpack representation over CONUS*

To better assess drought based on the soil moisture from LBS, it is first essential to ensure realistic representation of the snowpack itself. A 5-yr evaluation period from October 1994 to September 1999 (or WYs 1995–99), which is different from the calibration period (WYs 1985–89), is used to compare the SWE results from LBS forced with the default CPC data (denoted as LBS), LBS forced with PRISM data [denoted as LBS (PRISM)], and Noah NLDAS-2 outputs against the UA SWE dataset.

Figures 3a–d show that generally, LBS (PRISM) shows a better performance than Noah/NLDAS-2, with much more limited areas of large root mean squared errors (RMSEs) and biases. For instance, the number of grid boxes with RMSE values greater than 100 mm are 513 and 2136 for LBS (PRISM) and Noah/NLDAS-2, respectively. RMSE is much smaller for LBS (PRISM), particularly over regions such as the Rockies, though Noah performance is slightly better over the Northeast. LBS (PRISM) exhibits a positive bias over the majority of the country where the maximum daily climatological SWE is higher than 100 mm (Fig. 1), with the highest values over the Cascades. Noah/NLDAS-2 SWE demonstrates a prevalent negative bias, with greater magnitudes than LBS over the Rockies, Cascades, and Sierra Nevada. Replacing the PRISM P and T (used to develop the LBS) by the CPC P and T (used operationally in the CPC, not used in the LBS development), the LBS results still show an improved spatial representation of SWE over the Noah/NLDAS-2 (Figs. 3e,f), although some degradation is found, as expected, when compared to LBS (PRISM). This demonstrates that the scheme can produce reliable results with different datasets.

Time series of areal average SWE over the WEST domain (Fig. 4a) show that both LBS simulations (CPC and PRISM forcing data) present a closer fitting to the UA SWE than the Noah/NLDAS-2, with much smaller RMSEs from LBS forced with PRISM (6.6 mm) and with CPC (7.9 mm) than from the Noah/NLDAS-2 (25.1 mm). For New Hampshire (representing the East, Fig. 4b), both LBS results tend to overestimate SWE, while Noah-NLDAS2 shows an underestimation. The RMSE values from LBS simulations (38.0 and 42.7 mm, for CPC and PRISM forcing) are higher than these from Noah/NLDAS-2 (27.8 mm). In contrast, the temporal variability is better represented by both LBS simulations, with correlation coefficients of 0.97 for both, versus 0.89 for Noah/NLDAS-2. Other states were also analyzed, with consistently better performance than Noah/NLDAS-2 in the west, while comparable in the east. For instance, for Michigan, the RMSE values from LBS (PRISM), LBS, and Noah/NLDAS-2 are 11.4, 24.4, and 16.7 mm, respectively.

The differences in SWE between both LBS simulations (i.e., forced with CPC and PRISM data), are mainly driven by the T and P differences in the forcing datasets (Fig. S2). For the evaluation period (i.e., WYs 1995–99), the CPC forcing data show a wetter condition for most of the United States (but usually not surpassing 0.4 mm day^{-1} of mean difference) than the PRISM dataset (Fig. S2a). However, a drier condition over the mountainous areas is observed, with mean differences as large as −1.5 mm day^{-1} over Sierra Nevada and the Cascade Mountains. For temperature (Fig. S2b), the CPC dataset exhibits a warmer mean condition than the PRISM data over most of the western United States (up to 3°C for some areas), with a few spots over portions of the western mountains with the opposite behavior. In terms of root-mean-squared difference (RMSD), the largest differences in precipitation are found over the Cascades and Sierra Nevada, followed by the northern Rockies (Fig. S2c). The largest RMSDs for temperature are found in the intermountain region and to the east of the Rockies (Fig. S2d). These disparities are consistent with the differences in SWE between both LBS simulations shown in Fig. 3.

To expand the evaluation, a comparison of SWE from LBS, LBS (PRISM), and Noah/NLDAS-2 against SWE point observations from the SNOTEL stations is shown in Fig. S1 for the period WYs 2006–10. The median (mean) correlation coefficient across the more than 650 compared points is 0.89 (0.83) for both LBS and LBS (PRISM) (Figs. S1c,d), while the RMSE is 119 mm (172 mm) for LBS and 114 mm (175 mm) for LBS (PRISM). These results are better than those for the Noah/NLDAS-2 (Fig. S2b) with the median (mean) correlation being 0.65 (0.61) and the RMSE 153 mm (203 mm).

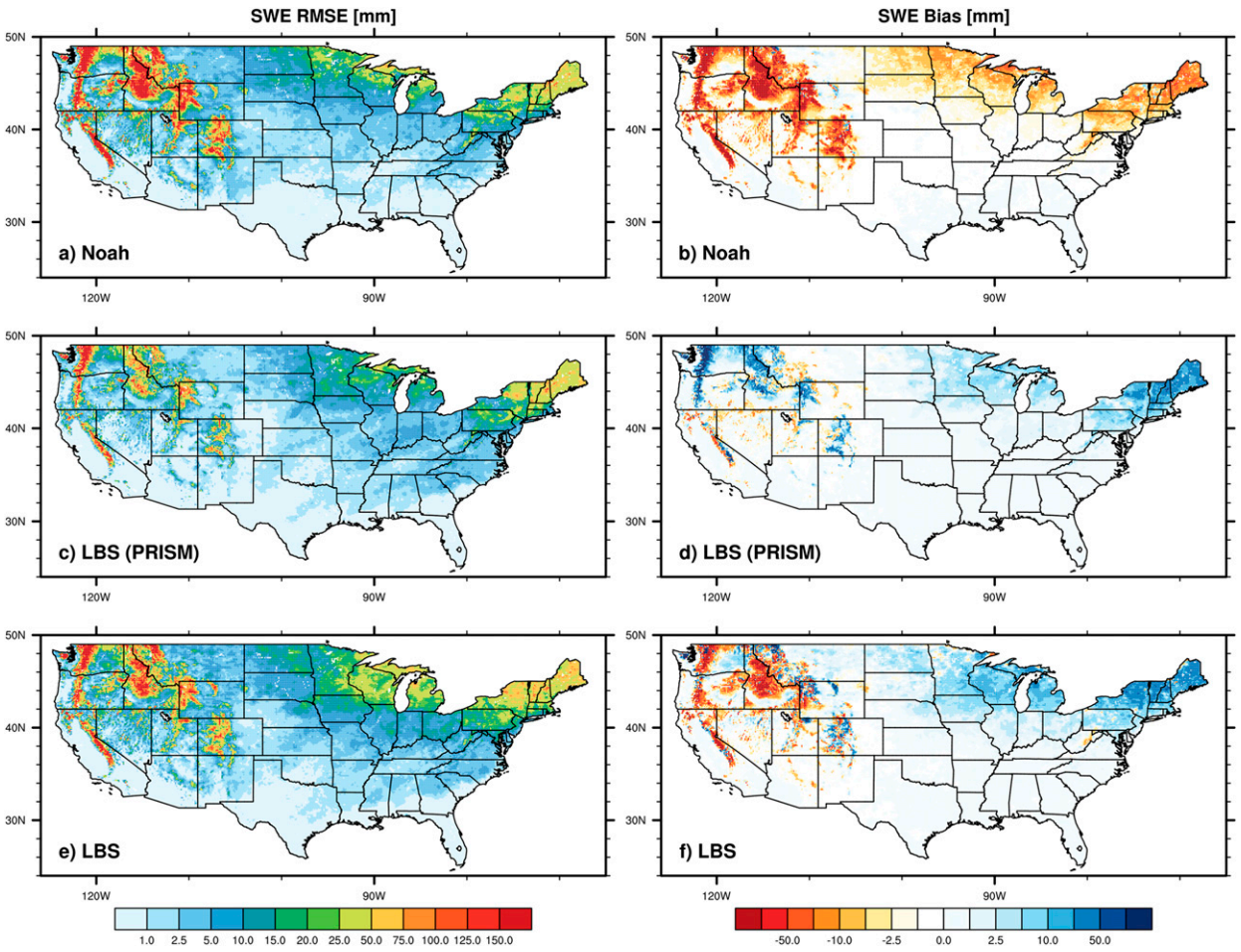

FIG. 3. Spatial performance of SWE from LBS and Noah/NLDAS-2. Map of (left) RMSE and (right) bias of SWE from (a),(b) Noah/NLDAS-2, (c),(d) LBS forced with PRISM, and (e),(f) LBS forced with CPC relative to the UA SWE, using all daily values from WYs 1995 to 1999.

Furthermore, the correlations in about 80% of the SNOTEL points are higher for LBS than for Noah/NLDAS-2, and in about 84% of the points for LBS (PRISM) (Fig. S1e). Similar proportions of lower RMSE for LBS and LBS (PRISM) versus Noah/NLDAS-2 are observed (Fig. S1f). For reference, the UA SWE product shows the best performance (Fig. S1a) with a median (mean) correlation of 0.92 (0.86) and RMSE of 105 mm (150 mm).

b. *Impacts of snow on soil moisture*

As our snowpack treatment is developed for the CPC operational implementation, only the simulations with the CPC forcing data are analyzed here. As the LB soil moisture was evaluated before (Fan and van den Dool 2004), here we focus on the snowpack effect on soil moisture (Fig. 5). At the beginning of the water year (1 October; top row of Fig. 5), snowmelt from the previous season leads to more soil moisture in LBS than in LB over the mountainous areas in the western United States.

During winter (1 January; second row of Fig. 5), snow coverage and snow water equivalent increase. Hence, LBS shows considerably less soil moisture than LB in the snowy areas, because snowfall is stored in the snowpack, not reaching the soil. By 1 April (third row of Fig. 5), snow coverage extent has decreased from that in January; however, SWE over the mountains and in the Northeast is close to its annual maximum. Accordingly, the soil moisture differences in such areas increased to be as large as 100 mm in magnitude, although covering a smaller area of the United States. As the melting season develops, the soil moisture differences between LBS and LB decrease in magnitude, due to water previously stored in the snowpack now reaching the soil. By 1 July (bottom row of Fig. 5), the increase in soil moisture due to snowmelt in the LBS is evident. This increased soil moisture lasts until the beginning of the next water year in some areas.

These results demonstrate the expected decrease in soil moisture during winter and increase in spring and summer due to water storage in the snowpack. Next, we will address how this impacts the drought assessment.

c. *Impacts on drought assessment*

For drought assessment, the standardized anomalies (SDAnoms) of soil moisture (with the threshold values provided

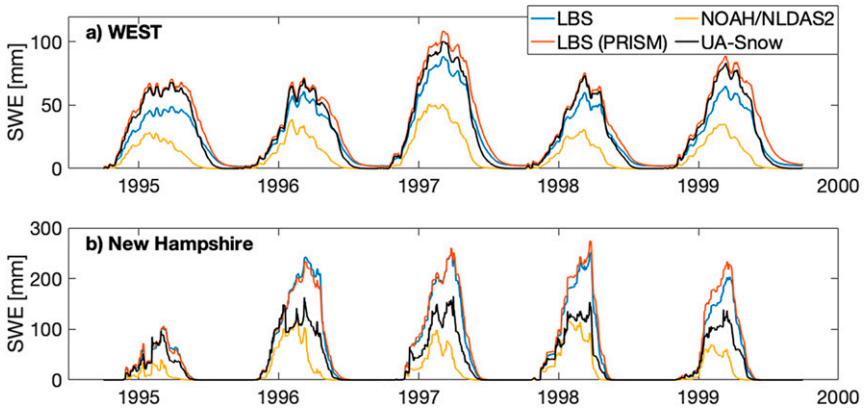

FIG. 4. Temporal variability of SWE from the LBS and Noah/NLDAS-2 models. Temporal evolution of areal average time series of SWE from LBS, LBS (PRISM), UA-SWE, and Noah/NLDAS-2 from 1 Oct 1994 to 30 Sep 1999, over (a) the WEST United States and (b) New Hampshire.

in section 2c) have been used as a proxy for the drought condition at CPC. We use the same approach here for comparison with the much more complex subjective analysis from the U.S. Drought Monitor. As the U.S.-DM data are available only since 1 January 2000, the period covered in this analysis is 1 January 2000–31 December 2016.

LB is able to reasonably simulate the temporal evolution of area percentages with different drought intensities over CONUS compared with U.S.-DM (Fig. 6a), with temporal correlations for categories D0–D4 being 0.64, 0.61, 0.59, 0.55, and 0.42, respectively. This supports the choice of such thresholds of SDAnoms as a surrogate for the drought condition. The temporal correlations between LBS and U.S.-DM are similar (0.63, 0.62, 0.61, 0.57, and 0.40). Figure 6b shows the differences between the percentage of covered areas mimicked by LBS and LB within each category (the five colored rows on the *y* axis, from D0 at top to D4 at bottom), as a function of time (horizontal axis). Differences as large as 5% of the entire CONUS area (dark red or dark blue) are seen for some categories. Such changes are larger during the winter and spring seasons, with some of them lasting longer, consistent with the snow season.

As the threshold selection is just informative, a more quantitative analysis is performed directly using the SDAnoms of soil moisture in Fig. 6c. As expected, the largest values of both mean difference and RMSD are found in the snow accumulation and melting seasons (winter and spring/summer). Here, the correlation between mean areal SWE anomalies over CONUS (red line in Fig. 6b) and the mean difference of SM SDAnoms is −0.86, aligned with the expectation of improved drought condition in LBS (compared to LB) for years with above normal SWE, and vice versa.

The spatial distribution of the temporal pixel-by-pixel RMSD and mean differences (LBS-LB) of the standardized soil moisture anomalies from both versions of the model are shown in Fig. 7. The RMSD (Fig. 7a) shows a similar spatial pattern to the climatological maximum SWE (Fig. 1), with high values over the mountainous areas over the western United States. This pattern highlights the importance of snowpack as a modulator of the annual cycle of the water balance variables, with meaningful changes in soil moisture over the snowy areas. The mean differences between LBS and LB are generally small in magnitude over most of the areas (mostly ranging between −0.1 and +0.1 SM standard deviations), with negative differences (meaning drier in LBS) over the Rockies and Sierra Nevada mountains, and positive differences (meaning wetter in LBS) over the Cascades and the northeast United States (Fig. 7b).

d. Case studies: Water years 2010 and 2013

To better understand the snowpack impacts on drought assessment, a more detailed analysis of different seasons was performed over the entire CONUS for WYs 2010 (here) and 2013 (in the supplemental material, including Fig. S3). Figure 6a shows that droughts were mostly localized and had relatively low intensity over CONUS in WY 2010, while larger portions of the United States were under drought conditions, including large areas under the most severe categories of drought, during WY 2013. These two years also show important differences in the mimicked drought categories simulated by LBS and LB (Figs. 6b,c). LBS shows less area in the categories D0 and D1 than LB for WY 2010 and more area in all the categories during WY 2013.

During early February 2010 (Fig. 8, left column), snowpack was widespread over the United States, with negative SWE anomalies over the Cascades and the Rockies (reaching up to −100 mm) and northeast United States. In contrast, the Sierra Nevada, the Utah–Arizona border, and the northern Great Plains showed positive SWE anomalies. The negative SWE anomalies in the West are consistent with the widespread abnormally dry area (D0) in the U.S.-DM, and so are those in the northern portions of Minnesota and Wisconsin (Fig. 8d). Overall, the original LB captures the general pattern of drought condition over most of the United States (Fig. 8g). However, it shows a severe deficit of soil moisture in the northern border between Idaho and Montana, inconsistent with the U.S.-DM, it does not identify the severe drought (D2) condition in northern Arizona/southern Utah, and it overestimates

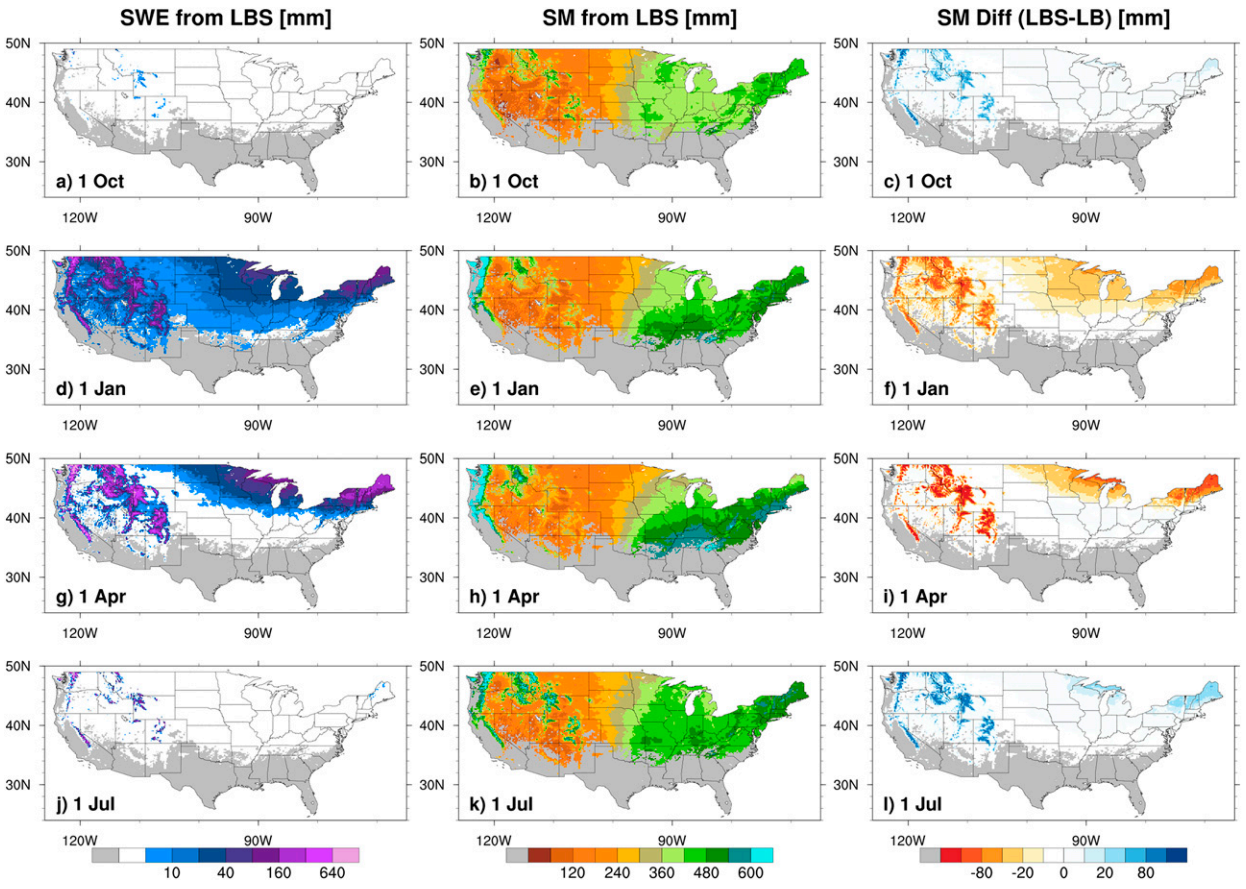

FIG. 5. Impact of snow treatment on LB-simulated soil moisture. Daily climatology of (left) snow water equivalent, (center) soil moisture from LBS, and (right) soil moisture difference between LBS and LB on (a)–(c) 1 Oct, (d)–(f) 1 Jan, (g)–(i) 1 Apr, and (j)–(l) 1 Jul. Climatology was computed between 1 Jan 1982 and 31 Dec 2016. Grays areas are masked out as in Fig. 1.

the drought condition in the Michigan/Indiana/Ohio region. With the snowpack treatment, LBS results are more consistent with the U.S.-DM, particularly over Nevada, Montana, and the eastern United States (Fig. 8m). For the northern Arizona/southern Utah area, the direction of the change is correct though too high, leading to an overestimation of the drought severity.

In early April (Fig. 8, center column), the negative anomalies of SWE expanded to most of the United States, except over the high elevations in the southern Rockies and Sierra Nevada (Fig. 8b). The largest changes in the U.S.-DM analysis with respect to early February are the increase in the drought severity over the borders of Northern California and Nevada, in part of the northern Rockies, as well as in the northern portions of Michigan, Pennsylvania and New York (Fig. 8e). The original LB overestimates the intensification over the northern Rockies and northeast United States, including the Great Lakes area, but represents quite well the condition on the California–Nevada border (Fig. 8h). The large SDAnoms differences between LBS and LB lead to a closer drought estimation of LBS (Fig. 8n) to the U.S.-DM than the original LB, although some differences still remain, most notably in Ohio and Kentucky.

In early June (Fig. 8, right column), after the melting season ended in most of the United States, negative anomalies of SWE still remained in parts of the Cascades and northern Rockies, while positive SWE anomalies persisted over the Sierra Nevada and part of the Rockies (Fig. 8c). The drought condition in the U.S.-DM worsened over the eastern United States but improved in the intermountain areas between the Rockies and the Cascades/Sierra Nevada (Fig. 8f). LB shows similar but amplified changes and it does not identify most of the Vermont/New Hampshire/Maine areas in any drought category (Fig. 8i). LBS in Fig. 8o shows slightly lower SDAnoms in the easternmost part of the United States and larger ones over mountainous areas in the West, making the simulated drought conditions in the West (particularly over the northeastern portion of Wyoming) and in the easternmost United States slightly better.

Due to the lack of horizontal flow between grid cells in LB/LBS, cells downstream of snowy areas do not benefit from the introduced SWE representation and its meltwater runoff. However, a subjective analysis of SWE anomalies can improve the overall drought assessment, like that performed by the U.S.-DM experts. As an example, no drought was identified in the northeastern United States during February and only small portions during April by the U.S.-DM (Figs. 8d,e). However, the large negative anomalies of SWE during early April

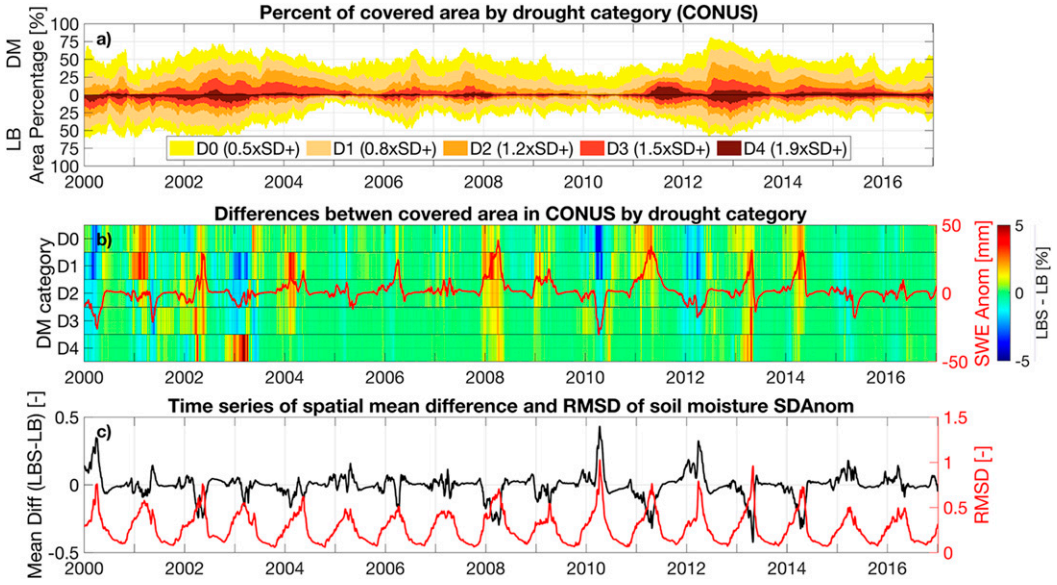

FIG. 6. Impacts of the snow treatment in the Leaky Bucket model on drought assessment. (a) Time series of the percentage area of CONUS in each drought category of the U.S. Drought Monitor (top) and the mimicked equivalent time series from the standardized soil moisture anomalies in the LB simulation (bottom). (b) Differences in the time series of percentage of covered area in the mimicked drought categories from LBS minus LB (five colored rows, with category D0 at the top and D4 at bottom); areal averaged SWE anomalies from LBS over CONUS are superimposed (red line, right axis). (c) Time series of spatial mean difference (black line; left axis) and RMSD (red line; right axis) of standardized soil moisture anomalies (LBS − LB) over CONUS.

(Fig. 8b) probably contributed to a drier condition during the following summer, coincident with the large D0 area identified for the northeast in June (Fig. 8f). Conversely, the positive SWE anomalies over Sierra Nevada probably helped to mitigate the dry condition in central California. This drought/SWE dynamic is better captured by LBS (Figs. 8m–o) than by the original LB (Figs. 8g–i).

For WY2013 (supplementary discussion S1 and Fig. S3), the addition of snowpack treatment led to a better representation of the drought condition over the mountainous areas in the West and in eastern United States, although it introduced some overestimation of the drought condition in the northern Great Plains.

4. Further discussion

As LBS includes the explicit representation of all relevant components of the water balance of a soil bucket (precipitation, snowpack, evapotranspiration, surface and subsurface runoff, and groundwater loss) and does not include arbitrary geographical or climatological considerations, it is expected to be applicable over CONUS and globally. Indeed, we have conducted the preliminary analysis of global application of LBS, finding that spatial and temporal variability of snowpack is adequately represented. Figure S4 shows that the snowpack impacts on soil moisture seasonality over the Northern Hemisphere are consistent with those presented for CONUS. More detailed analysis is being conducted for future work.

It is important to note that because of its many simplifications (e.g., single-layer soil, no energy balance considerations, no diurnal cycle, etc.), LBS is not appropriate for hydrological simulations in general (e.g., streamflow), land surface modeling or land-atmosphere coupled modeling where both land surface water and energy balances must be maintained (which can be done by complex LSMs only, such as Noah). However, the improved performance of LBS compared to Noah in simulating SWE suggests that further evaluation of Noah snowpack simulations (e.g., following the analysis in Fig. 2) will be helpful for Noah model improvement. Furthermore, reasonable agreement of LBS with the drought condition from the U.S. Drought Monitor and its consistency when forced with different datasets justifies its usage for both drought monitoring (using observation-based temperature and precipitation data) and prediction (using postprocessed temperature and precipitation data from numerical models for daily to seasonal forecasts).

Furthermore, LBS can be a useful tool to stakeholders, as the analysis of SM and SWE values and anomalies will provide information not only on the current water availability within the soil, but also the water storage in the snowpack that can inform water availability during and after the melting season. For example, this can help reservoir managers to balance the need of maximizing the water storage to satisfy the requirements of their users, against the safety measure of leaving capacity to avoid overflows, and to reduce the uncertainty in the spring/summer inflows (Harpold et al. 2017a). An analysis of SWE can also help to inform the wildfire stakeholders, as an early snowmelt has been associated to increased wildfire risk in the following seasons (Westerling et al. 2006).

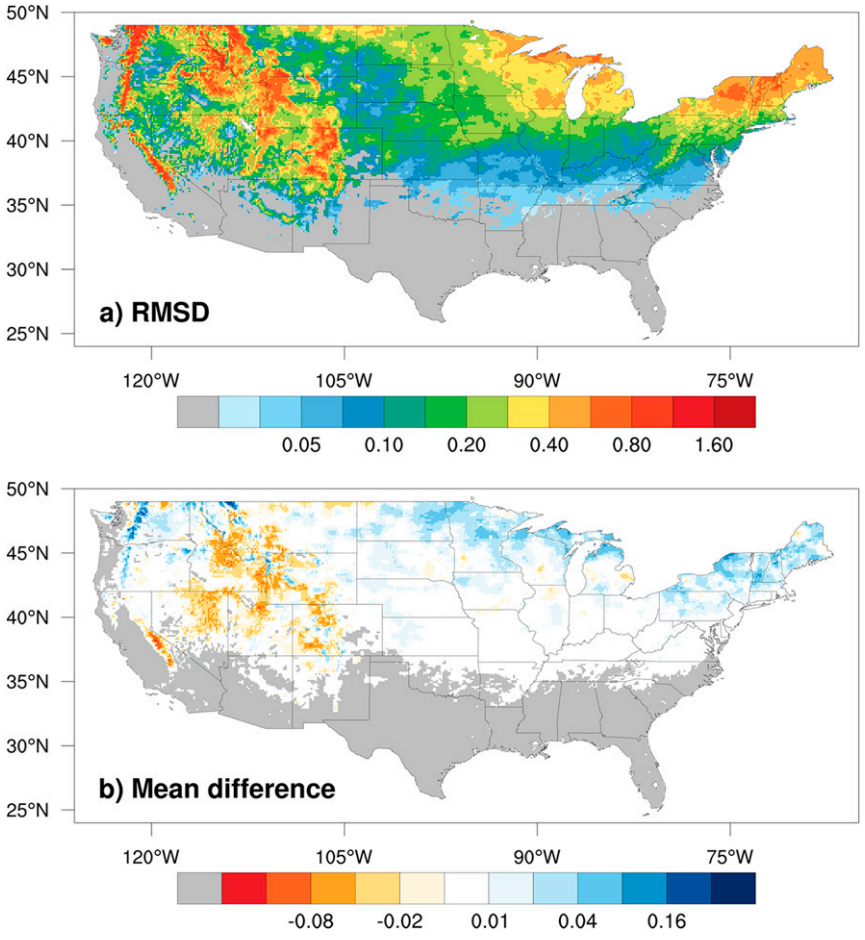

FIG. 7. Maps of the temporal RMSD and mean difference of soil moisture standardized anomalies. (a) Map of the RMSD and (b) map of the mean difference (LBS − LB), computed pixel by pixel for the period 1 Jan 2000–31 Dec 2016.

On the other hand, the uncertainties associated with LBS and discussed in section 2b must be carefully considered. In particular, the lack of lateral flow between grid cells prevents the model from spreading the benefits of a reliable snow representation to the downstream valleys. Furthermore, as our development of the snow scheme is based on pixels with an average of at least 20 days per year of snow cover, relative uncertainties are expected to be larger over areas with intermittent snow coverage.

5. Conclusions

We have developed a simple one-layer snow scheme for implementation in the CPC Leaky Bucket (LB), currently used to postprocess temperature and precipitation for operational drought assessment through analysis of soil moisture anomalies. This snow treatment introduces SWE as an additional prognostic variable, and both this scheme and LB are driven by daily precipitation and temperature data only. Although simple, LB with the snow treatment (i.e., LBS) accounts for most of the water balance processes, allowing for a more comprehensive drought assessment than the commonly used indices (e.g., SPI or PDSI), without requiring a large suite of variables used in more recent indices (e.g., SZI).

LBS performs well against the UA SWE dataset (e.g., RMSE of ~7 mm over the West United States; Figs. 3 and 4) and SNOTEL observations (e.g., median correlation among the more than 650 stations of 0.89; Fig. S1). In particular, the simple LBS performs better than a complex LSM (Noah/NLDAS-2) in both spatial and temporal SWE variability when forced with the PRISM or CPC data (based on the NLDAS-2 forcing data), supporting its usability with different datasets. Hence the snowpack treatment in the LBS adds a new advantage to the CPC efforts in drought assessment, as it provides the valuable output of a reliable SWE and its anomalies that could also be used to further improve the multivariable analysis of droughts.

As expected, snowpack changes the soil moisture seasonality in the model. First, snowpack decreases soil moisture over snow-covered areas in winter due to snowfall/water storage in the snowpack (rather than reaching the soil), even counteracting the snowpack's inhibition of evapotranspiration. The stored water in

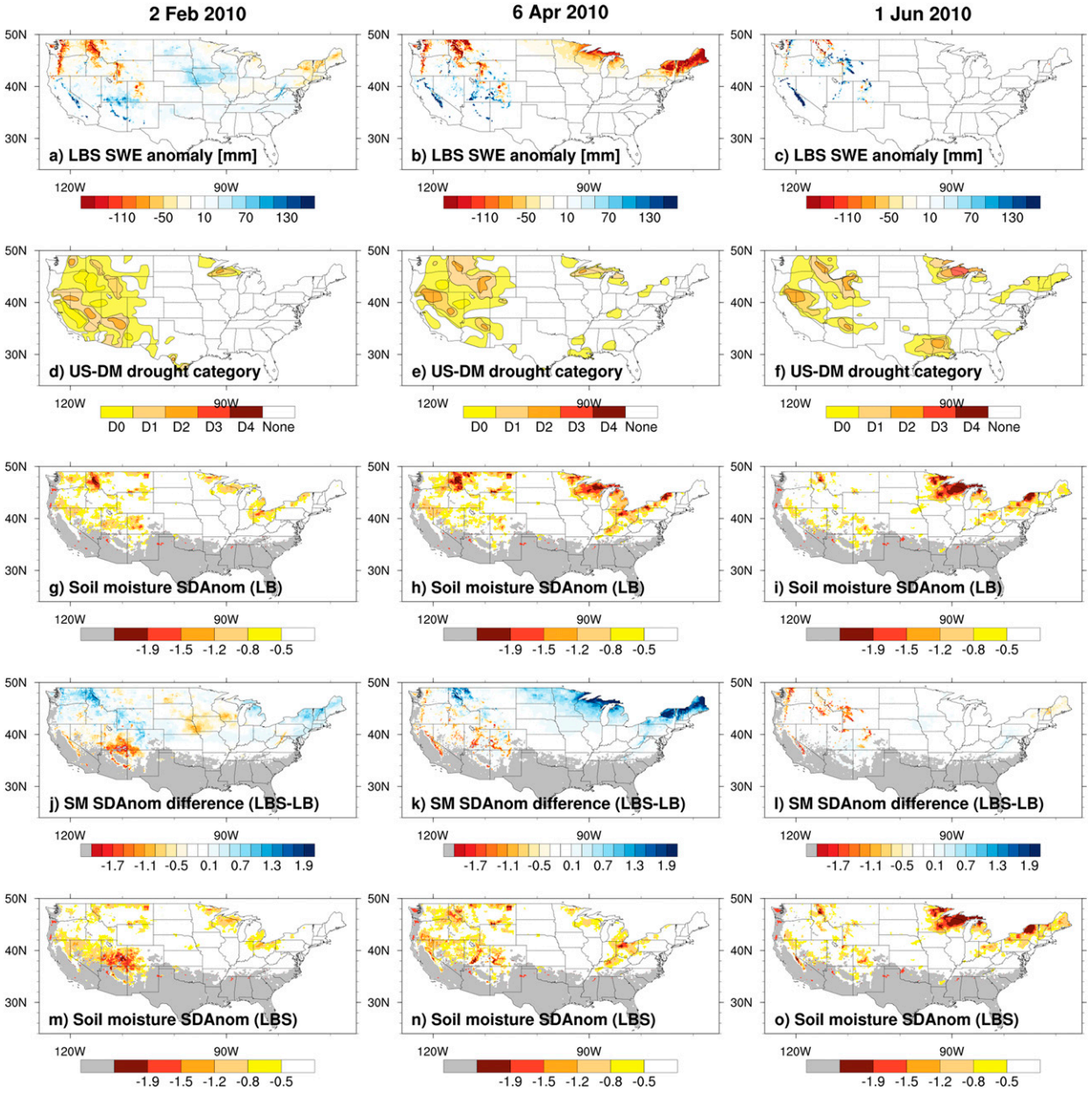

FIG. 8. Impact of snow treatment in LBS on the drought condition in WY 2010. Maps of (a)–(c) SWE anomalies, (d)–(f) areas under the five categories in the U.S. Drought Monitor, (g)–(i) SDAnoms of soil moisture from the LB (colored by the mimicked thresholds for the DM categories), (j)–(l) difference in SDAnoms of soil moisture (LBS-LB), and (m)–(o) the SDAnoms of soil moisture from LBS in early (left) February, (center) April, and (right) June when the U.S.-DM data were available.

the snowpack becomes available in the melting season, increasing soil moisture. Over mountainous areas, the snowpack impact on soil moisture can carry over to the following Water Year.

Compared with the U.S.-DM data, our snowpack treatment improves the LB simulation of the temporal and spatial distribution of drought conditions overall (Fig. 8 and Fig. S3). This justifies an increased confidence in the drought assessment derived from the Leaky Bucket postprocessing over snow-covered regions. This will contribute to the drought assessment, as the soil moisture anomalies from LBS represent the contribution of CPC to the multiagency U.S. Drought Monitor. Because of the results reported in this study, our snowpack scheme has been implemented in the CPC operational LBS runs, and results are freely available at https://www.cpc.ncep.noaa.gov/products/Soilmst_Monitoring/index.shtml. Furthermore, an expert subjective analysis of both SM and SWE can inform stakeholders not only about the current drought status, but also about the expected spring/summer drought condition

during and after the melting season for snow dominated basins.

Acknowledgments. This work was supported by the NOAA National Weather Service (NA18NWS4680061) and the U.S. Army Corps of Engineers via the Center for Western Weather and Water Extremes at Scripps Institution of Oceanography (W912HZ-15-2-0019). We thank Jorge Mora for providing shapefiles for the domains and Michael A. Brunke for careful proofreading. We also thank the Editor (Matthew Rodell), Adrian Harpold, and two anonymous reviewers for insightful and constructive comments and suggestions. The authors declare that they have no conflict of interest.

Data availability statement. The UA SWE data are available at: https://nsidc.org/data/nsidc-0719, the PRISM temperature and precipitation data at: https://prism.oregonstate.edu/, the Noah/NLDAS-2 data at: https://disc.gsfc.nasa.gov/, and the U.S. Drought Monitor data at: https://droughtmonitor.unl.edu/. The snowpack treatment code is available from J.A. and the Leaky Bucket model (including the version with our snowpack treatment) is available from Y.F.

REFERENCES

Behrangi, A., X. Yin, S. Rajagopal, D. Stampoulis, and H. Ye, 2018: On distinguishing snowfall from rainfall using near-surface atmospheric information: Comparative analysis, uncertainties and hydrologic importance. *Quart. J. Roy. Meteor. Soc.*, **144**, 89–102, https://doi.org/10.1002/qj.3240.

Blahušiaková, A., M. Matoušková, M. Jenicek, O. Ledvinka, Z. Kliment, J. Podolinská, and Z. Snopková, 2020: Snow and climate trends and their impact on seasonal runoff and hydrological drought types in selected mountain catchments in Central Europe. *Hydrol. Sci. J.*, **65**, 2083–2096, https://doi.org/10.1080/02626667.2020.1784900.

Bloomfield, J. P., and B. P. Marchant, 2013: Analysis of groundwater drought building on the standardised precipitation index approach. *Hydrol. Earth Syst. Sci.*, **17**, 4769–4787, https://doi.org/10.5194/hess-17-4769-2013.

Broxton, P. D., N. Dawson, and X. Zeng, 2016a: Linking snowfall and snow accumulation to generate spatial maps of SWE and snow depth. *Earth Space Sci.*, **3**, 246–256, https://doi.org/10.1002/2016EA000174.

——, X. Zeng, and N. Dawson, 2016b: Why do global reanalyses and land data assimilation products underestimate snow water equivalent? *J. Hydrometeor.*, **17**, 2743–2761, https://doi.org/10.1175/JHM-D-16-0056.1.

——, ——, and ——, 2019: Daily 4 km gridded SWE and snow depth from assimilated in-situ and modeled data over the Conterminous US, version 1. NASA National Snow and Ice Data Center Distributed Active Archive Center, accessed 1 July 2019, https://doi.org/10.5067/0GGPB220EX6A.

Cho, E., J. M. Jacobs, and C. M. Vuyovich, 2020: The value of long-term (40 years) airborne gamma radiation SWE record for evaluating three observation-based gridded SWE data sets by seasonal snow and land cover classifications. *Water Resour. Res.*, **56**, e2019WR025813, https://doi.org/10.1029/2019WR025813.

Dai, A., and T. Zhao, 2017: Uncertainties in historical changes and future projections of drought. Part I: Estimates of historical drought changes. *Climatic Change*, **144**, 519–533, https://doi.org/10.1007/s10584-016-1705-2.

Daly, C., M. Halbleib, J. I. Smith, W. P. Gibson, M. K. Doggett, G. H. Taylor, J. Curtis, and P. P. Pasteris, 2008: Physiographically sensitive mapping of climatological temperature and precipitation across the conterminous United States. *Int. J. Climatol.*, **28**, 2031–2064, https://doi.org/10.1002/joc.1688.

Dawson, N., P. Broxton, and X. Zeng, 2017: A new snow density parameterization for land data initialization. *J. Hydrometeor.*, **18**, 197–207, https://doi.org/10.1175/JHM-D-16-0166.1.

——, ——, and ——, 2018: Evaluation of remotely sensed snow water equivalent and snow cover extent over the contiguous United States. *J. Hydrometeor.*, **19**, 1777–1791, https://doi.org/10.1175/JHM-D-18-0007.1.

Doesken, N. J., T. B. McKee, and J. Kleist, 1991: Development of a surface water supply index for the western United States. Final Rep., 84 pp.

Fan, Y., and H. M. van den Dool, 2004: Climate Prediction Center global monthly soil moisture data set at 0.5° resolution for 1948 to present. *J. Geophys. Res.*, **109**, D10102, https://doi.org/10.1029/2003JD004345.

——, and ——, 2011: Bias correction and forecast skill of NCEP GFS ensemble week-1 and week-2 precipitation, 2-m surface air temperature, and soil moisture forecasts. *Wea. Forecasting*, **26**, 355–370, https://doi.org/10.1175/WAF-D-10-05028.1.

——, ——, and W. Wu, 2011: Verification and intercomparison of multimodel simulated land surface hydrological datasets over the United States. *J. Hydrometeor.*, **12**, 531–555, https://doi.org/10.1175/2011JHM1317.1.

Harpold, A. A., M. Dettinger, and S. Rajagopal, 2017a: Defining snow drought and why it matters. *Eos, Trans. Amer. Geophys. Union*, **98**, 15–17, https://doi.org/10.1029/2017EO068775.

——, M. L. Kaplan, P. Z. Klos, T. Link, J. P. McNamara, S. Rajagopal, R. Schumer, and C. M. Steele, 2017b: Rain or snow: Hydrologic processes, observations, prediction, and research needs. *Hydrol. Earth Syst. Sci.*, **21**, 1–22, https://doi.org/10.5194/hess-21-1-2017.

Heim, R. R. J., 2002: A review of twentieth-century drought indices used in the United States. *Bull. Amer. Meteor. Soc.*, **83**, 1149–1166, https://doi.org/10.1175/1520-0477-83.8.1149.

Huang, J., H. M. van den Dool, and K. P. Georgakakos, 1996: Analysis of model-calculated soil moisture over the United States (1931-1993) and applications to long-range temperature forecasts. *J. Climate*, **9**, 1350–1362, https://doi.org/10.1175/1520-0442(1996)009<1350:AOMCSM>2.0.CO;2.

Huning, L. S., and A. AghaKouchak, 2020: Global snow drought hot spots and characteristics. *Proc. Natl. Acad. Sci. USA*, **117**, 19 753–19 759, https://doi.org/10.1073/pnas.1915921117.

Jenicek, M., J. Seibert, M. Zappa, M. Staudinger, and T. Jonas, 2016: Importance of maximum snow accumulation for summer low flows in humid catchments. *Hydrol. Earth Syst. Sci.*, **20**, 859–874, https://doi.org/10.5194/hess-20-859-2016.

Lloyd-Hughes, B., 2014: The impracticality of a universal drought definition. *Theor. Appl. Climatol.*, **117**, 607–611, https://doi.org/10.1007/s00704-013-1025-7.

McKee, T. B., N. J. Doesken, and J. Kleist, 1993: The relationship of drought frequency and duration to time scales. *Proc. Eighth Conf. on Applied Climatology*, Anaheim, CA, Amer. Meteor. Soc., 179–183.

Mishra, A. K., and V. P. Singh, 2010: A review of drought concepts. *J. Hydrol.*, **391**, 202–216, https://doi.org/10.1016/j.jhydrol.2010.07.012.

Mukherjee, S., A. Mishra, and K. E. Trenberth, 2018: Climate change and drought: A perspective on drought indices. *Curr. Climate Change Rep.*, **4**, 145–163, https://doi.org/10.1007/s40641-018-0098-x.

Narasimhan, B., and R. Srinivasan, 2005: Development and evaluation of Soil Moisture Deficit Index (SMDI) and Evapotranspiration Deficit Index (ETDI) for agricultural drought monitoring. *Agric. For. Meteor.*, **133**, 69–88, https://doi.org/10.1016/j.agrformet.2005.07.012.

NDMC/NOAA/USDA, 1999: U.S. Drought Monitor. Accessed 5 March 2020, https://droughtmonitor.unl.edu/.

Naumann, G., and Coauthors, 2018: Global changes in drought conditions under different levels of warming. *Geophys. Res. Lett.*, **45**, 3285–3296, https://doi.org/10.1002/2017GL076521.

Palmer, W. C., 1965: Meteorological drought. U.S. Weather Bureau Research Paper 45, 58 pp.

Petersky, R., and A. Harpold, 2018: Now you see it, now you don't: A case study of ephemeral snowpacks and soil moisture response in the Great basin, USA. *Hydrol. Earth Syst. Sci.*, **22**, 4891–4906, https://doi.org/10.5194/hess-22-4891-2018.

Samimi, S., and S. J. Marshall, 2017: Diurnal cycles of meltwater percolation, refreezing, and drainage in the supraglacial snowpack of Haig glacier, Canadian Rocky Mountains. *Front. Earth Sci.*, **5**, 6, https://doi.org/10.3389/feart.2017.00006.

Sheffield, J., G. Goteti, F. Wen, and E. F. Wood, 2004: A simulated soil moisture based drought analysis for the United States. *J. Geophys. Res.*, **109**, D24108, https://doi.org/10.1029/2004JD005182.

Staudinger, M., K. Stahl, and J. Seibert, 2014: A drought index accounting for snow. *Water Resour. Res.*, **50**, 7861–7872, https://doi.org/10.1002/2013WR015143.

Sutanto, S. J., M. van der Weert, N. Wanders, V. Blauhut, and H. A. J. Van Lanen, 2019: Moving from drought hazard to impact forecasts. *Nat. Commun.*, **10**, 4945, https://doi.org/10.1038/s41467-019-12840-z.

Svoboda, M., and Coauthors, 2002: The drought monitor. *Bull. Amer. Meteor. Soc.*, **83**, 1181–1190, https://doi.org/10.1175/1520-0477-83.8.1181.

Techel, F., and C. Pielmeier, 2011: Point observations of liquid water content in wet snow—Investigating methodical, spatial and temporal aspects. *Cryosphere*, **5**, 405–418, https://doi.org/10.5194/tc-5-405-2011.

The PRISM Climate Group, 2004: PRISM gridded climate data. Oregon State University, accessed 1 July 2019, http://prism.oregonstate.edu/.

Thomas, B. F., J. S. Famiglietti, F. W. Landerer, D. N. Wiese, N. P. Molotch, and D. F. Argus, 2017: GRACE groundwater drought index: Evaluation of California central valley groundwater drought. *Remote Sens. Environ.*, **198**, 384–392, https://doi.org/10.1016/j.rse.2017.06.026.

Trenberth, K. E., A. Dai, G. Van Der Schrier, P. D. Jones, J. Barichivich, K. R. Briffa, and J. Sheffield, 2014: Global warming and changes in drought. *Nat. Climate Change*, **4**, 17–22, https://doi.org/10.1038/nclimate2067.

van den Dool, H., J. Huang, and Y. Fan, 2003: Performance and analysis of the constructed analogue method applied to U.S. soil moisture over 1981–2001. *J. Geophys. Res.*, **108**, 8617–16, https://doi.org/10.1029/2002JD003114.

Van Loon, A. F., 2015: Hydrological drought explained. *Wiley Interdiscip. Rev.: Water*, **2**, 359–392, https://doi.org/10.1002/wat2.1085.

——, and H. A. J. Van Lanen, 2012: A process-based typology of hydrological drought. *Hydrol. Earth Syst. Sci.*, **16**, 1915–1946, https://doi.org/10.5194/hess-16-1915-2012.

Wang, W., M. Chen, and A. Kumar, 2010: An assessment of the CFS real-time seasonal forecasts. *Wea. Forecasting*, **25**, 950–969, https://doi.org/10.1175/2010WAF2222345.1.

Wang, Y.-H., P. Broxton, Y. Fang, A. Behrangi, M. Barlage, X. Zeng, and G.-Y. Niu, 2019: A wet-bulb temperature-based rain-snow partitioning scheme improves snowpack prediction over the drier western United States. *Geophys. Res. Lett.*, **46**, 13 825–13 835, https://doi.org/10.1029/2019GL085722.

Westerling, A. L., H. G. Hidalgo, D. R. Cayan, and T. W. Swetnam, 2006: Warming and earlier spring increase western U.S. forest wildfire activity. *Science*, **313**, 940–943, https://doi.org/10.1126/science.1128834.

Wilhite, D. A., and M. H. Glantz, 1985: Understanding the drought phenomenon: The role of definitions. *Water Int.*, **10**, 111–120, https://doi.org/10.1080/02508068508686328.

Xia, Y., and Coauthors, 2009: NLDAS primary forcing data L4 hourly 0.125 × 0.125 degree V002 (NLDAS_FORA0125_H). NASA/GSFC/HSL Goddard Earth Sciences Data and Information Services Center, accessed 1 July 2019, https://doi.org/10.5067/6J5LHHOHZHN4.

——, and Coauthors, 2012a: NLDAS Noah Land Surface Model L4 hourly 0.125 × 0.125 degree V002 (NLDAS_NOAH0125_H). NASA/GSFC/HSL Goddard Earth Sciences Data and Information Services Center, accessed 23 August 2019, https://doi.org/10.5067/47Z13FNQODKV.

——, and Coauthors, 2012b: Continental-scale water and energy flux analysis and validation for the North American Land Data Assimilation System project phase 2 (NLDAS-2): 1. Intercomparison and application of model products. *J. Geophys. Res.*, **117**, D03109, https://doi.org/10.1029/2011JD016048.

Zeng, X., P. Broxton, and N. Dawson, 2018: Snowpack change from 1982 to 2016 over conterminous United States. *Geophys. Res. Lett.*, **45**, 12 940–12 947, https://doi.org/10.1029/2018GL079621.

Zhang, B., X. Zhao, J. Jin, and P. Wu, 2015: Development and evaluation of a physically based multiscalar drought index: The Standardized Moisture Anomaly Index. *J. Geophys. Res. Atmos.*, **120**, 11 575–11 588, https://doi.org/10.1002/2015JD023772.

——, Y. Xia, L. S. Huning, J. Wei, G. Wang, and A. AghaKouchak, 2019: A framework for global multicategory and multiscalar drought characterization accounting for snow processes. *Water Resour. Res.*, **55**, 9258–9278, https://doi.org/10.1029/2019WR025529.